Phosphatidylserine polarization is required for proper Cdc42 localization and for development of cell polarity.

Gregory D. Fairn[1] and Sergio Grinstein[1]

[1]Program in Cell Biology, Hospital for Sick Children,

Toronto, ON, Canada M5G1X8

Keywords: cell polarity; phosphatidylserine; Cdc42; membrane diffusion

Address correspondence to: Sergio Grinstein
Program in Cell Biology,
The Hospital for Sick Children,
555 University Avenue,
Toronto, Ontario,
Canada M5G 1X8,
Tel: (416) 813-5727; Fax: (416) 813-5028
Email: sergio.grinstein@sickkids.ca

SUMMARY

We used genetically-encoded fluorescent probes to visualize the distribution of phosphatidylserine (PS) in live *S. cerevisiae*. The majority of the PS was found to reside in the cytosolic leaflet of the plasma membrane. Remarkably, PS was polarized, accumulating in bud necks, the bud cortex and the tips of mating projections. Polarization required vectorial delivery of PS-enriched secretory and recycling vesicles. Rapid dissipation of the PS gradient is prevented by the slow diffusion of lipids along the plasmalemmal inner leaflet, estimated by photobleaching recovery measurements to be over an order of magnitude slower than in mammalian cells. In mutants lacking PS-synthase the absence of PS was associated with, and likely responsible for impaired polarization of the Cdc42 complex, leading to inhibition of bud emergence, diminished growth rate and abolishment of mating. The results indicate that PS polarization is required for optimal Cdc42 targeting and activation during cell division and mating.

The establishment of polarity is key to cellular replication and to the development and function of multicellular organisms. Because they are genetically tractable, yeast have become a useful model for the study of cell polarity. Recent studies revealed that in *S. cerevisiae* the small GTPase Cdc42 is a pivotal regulator of polarity, a conclusion that has been extended to other eukaryotic organisms [1]. In yeast, Cdc42 along with Cdc24 are enriched at the incipient bud site and at the tip of the mating projections that form in response to pheromones [2,3]. As for other Rho-family GTPases, the activity of Cdc42 is dictated by its degree of GTP-occupancy, and stimulation of nucleotide exchange initiates polarization of the actin cytoskeleton at presumptive bud sites or in response to mating pheromones [4]. Positive feedback loops then contribute to bud emergence. Several factors, including actin cables and the adaptor protein Bem1, appear to influence or stabilize these loops by aiding in the delivery and retention of Cdc42 and its effectors [3,5-7].

Upon the establishment of a polarity axis the cellular machinery is able to vectorially target secretion, resulting in a polarized distribution of specific plasma membrane proteins such as Snc1 and Fus1 [8,9]. The polarization of proteins can then be maintained by a diffusion barrier and/or by selective endocytosis and directed recycling. In the case of Snc1, a yeast synaptobrevin homologue, selective endocytosis is followed by recycling back to the membrane via the secretory pathway [9]. Additionally, fluorescent recovery after photobleaching (FRAP) experiments demonstrated that Snc1 has a low lateral diffusion rate, which helps maintain its polarization [9]. Conversely Fus1, a fusion protein, appears to be retained at the tips of mating projections through protein-protein interactions and is not reliant on recycling [8].

Like proteins, lipids also have the ability to spatially and temporally regulate important events such as cell migration and endocytosis. Some phospholipids, like phosphatidylserine (PS), show marked asymmetry in their distribution between and across membranes. While it comprises only 3-10% of the phospholipids in eukaryotic cells, PS is enriched in the plasma membrane, where it is found almost exclusively in the inner leaflet [10]. In mammalian cells the

cytosolic leaflet of the plasmalemma is composed of ~20-30% PS and the fraction has been estimated to be even higher in yeast, reaching 50-60% [11,12]. Yet, aside from its appreciated roles in the clearance of apoptotic bodies and blood coagulation, the biological functions of PS and the significance of its asymmetric distribution are poorly understood. Particularly little is known about the role of PS in cell polarization and replication. In yeast, PS levels show peak concentrations at the time of bud emergence, followed by a decrease through the remainder of the cell cycle [13]. This contrasts with the behavior of phosphatidylcholine (PC) and phosphatidylethanolamine (PE), which increase linearly in abundance as the cell cycle progresses [13]. This differential behavior is reflected in the cellular PC:PS ratio, which is ≈2:1 at the time of bud emergence, while at later stages of the cell cycle it approaches 6:1. The functional significance of these drastic changes has not been explored.

Progress in understanding PS physiology has been hampered by our inability to visualize this phospholipid inside live cells. This limitation was recently overcome by the development of fluorescent PS biosensors based on the ability of the discoidin C2 domain to selectively recognize PS [14]. Using one such genetically-encoded biosensor we show here not only that PS accumulates preferentially in the plasma membrane of *S. cerevisiae* but, surprisingly, that it is unevenly distributed within the plasma membrane. Specifically, PS was found to accumulate markedly at budding sites and in mating projections. We proceeded to study the mechanism underlying the polarized distribution of PS and its potential significance to the budding and mating processes. Using a variety of traffic- and PS synthase-deficient mutants we concluded that targeted secretion is largely responsible for the polarization of PS and that this, in turn, is required for the localized recruitment of Cdc42 and its associated proteins, and for optimal cell replication and mating.

RESULTS

Phosphatidylserine distribution.

We used the GFP-Lact-C2 probe [14] to visualize the intracellular distribution of PS in *S. cerevisiae*. This genetically-encoded biosensor is expressed in the cytosol and therefore detects only PS on the cytosolically-exposed surfaces of organelles. As found in mammalian cells [14], the PS probe accumulated in the plasma membrane of yeast with no detectable signal in the endoplasmic reticulum or mitochondria, which are sites of PS synthesis and decarboxylation, respectively. However, unlike mammalian cells, little probe was associated with the yeast endosomes or vacuole/lysosomes (Fig. 1a). This may reflect a greater PS concentration difference between the plasma membrane and endocytic organelles in the case of yeast; in *S. cerevisiae* PS comprises ≈34% of the plasma membrane lipid, but <5% of the vacuolar lipid [11].

Because an earlier report had described an increased PS content at the time of bud emergence, we more closely examined PS distribution during the cell cycle. At all stages of the cell cycle the fluorescence of GFP-Lact-C2 was largely confined to the plasma membrane. However, the probe showed differential accumulation in distinct regions of the membrane depending upon the stage of the cycle (Fig. 1a,d). PS was concentrated at incipient bud sites (stage i in Fig. 1) and in small buds (stage ii). As the cells progress through the cell cycle and the bud becomes larger, increased signal is seen at the bud neck and the bud itself is enriched in PS compared to the mother cell (stages iii and iv). In contrast, the distribution of phosphatidylinositol 4,5-*bis*phosphate (PI4,5P_2), monitored using two tandem PH-domains of PLCδ fused to GFP, showed only modest polarization during the cycle (Fig. 1b,d), consistent with previous findings [15]. PI4,5P_2 accumulated ≈30% in the bud cortex and neck compared to the remainder of the mother cell. In comparison, the PS signal was increased by 236% in the bud cortex and 338% at the bud neck.

We also used GFP-Ras2 as a marker to ensure that the observed differences in fluorescence were not caused by increased membrane density. Like the homologous metazoan N-Ras proteins, yeast Ras2 is post-translationally processed by addition of palmitoyl and farnesyl moieties [16]. These hydrophobic modifications target Ras2 to the plasmalemma, where it can be used to assess membrane density [17]. As shown in Fig. 1c, Ras2 is rather evenly distributed throughout the membrane at all stages of the cycle. Together, these results demonstrate that PS enrichment at the site of bud formation is not an artifact generated by sub-microscopic membrane infolding, nor is it a general property of plasma membrane lipids or lipid-modified plasmalemmal proteins.

Secretion is required to polarize PS

PS biosynthesis takes place in the endoplasmic reticulum. By mechanisms that are incompletely understood, PS is subsequently delivered to other cellular organelles, including the plasma membrane [10,12,18]. It was therefore conceivable that the PS found to accumulate at bud sites originated from the secretory pathway. Indeed, in growing yeast exocytosis is known to be preferentially directed to sites of bud formation [19,20]. We took advantage of temperature-sensitive mutants to investigate the role of secretion in generating the polarized distribution of PS. Sec1, a founding member of the Sec1/Munc-18 family of proteins, and Sec6, an exocyst component, are both involved in the delivery of secretory vesicles to the plasma membrane [21]. We monitored the effects of *SEC1* and *SEC6* mutants on the distribution of PS and, for comparison, also examined the distribution of the yeast synaptobrevin homologue, Snc1. Snc1 continually cycles between the Golgi and the plasma membrane via secretory vesicles [9,22,23]. In wild-type yeast at steady state GFP- or mRFP-tagged Snc1 is found primarily in the plasma membrane and is enriched in the bud, whether the cells are grown at 25°C or 37°C (Lewis et al., 2000; Fig. 2a). A similar distribution of GFP-Snc1 was noted in $sec1^{ts}$ or $sec6^{ts}$ cells grown at 25°C, the permissive temperature (Fig. 2a). When secretion is impaired by elevating the

temperature, *sec1*^{ts} and *sec6*^{ts} cells are known to accumulate both high- and low-density secretory vesicles near sites of exocytosis [22,24]. Accordingly, after incubation at 37ºC for 30 min, we found GFP-Snc1 to accumulate in vesicular structures at or near budding sites (Fig. 2a). Parallel experiments in cells expressing GFP-Lact-C2 showed that the *sec1*^{ts} and *sec6*^{ts} cells had a normal distribution of the PS probe at 25°C (Fig. 2b). In contrast, vesicles decorated with GFP-Lact-C2 were found to accumulate intracellularly as early as 10 min after shifting the temperature to 37ºC and most cells displayed multiple PS-enriched vesicles as well as net depletion and loss of polarity of plasmalemmal PS after 30 min (Fig. 2b). Together, these observations suggest that secretory vesicles contain PS on their cytosolic face and that exocytic delivery is required to establish PS polarization during budding.

To further investigate the role of the secretory pathway in the polarization of PS we took advantage of a temperature-sensitive mutation that blocks exit from the *trans*-Golgi. Sec7 is a nucleotide-exchange factor for Arf1/2, required for vesicular exit from the Golgi complex and hence for maintenance of proper Golgi morphology and function [25-27]. *Sec7*^{ts} cells were co-transformed with mRFP-Snc1 and GFP-C2-Lact and grown to early log phase at 25°C. Fig. 2c shows that at this permissive temperature mRFP-Snc1 is localized almost exclusively to the bud and GFP-C2-Lact is similarly polarized. Following incubation for 60 min at 37°C, however, Snc1 accumulated in internal structures identified earlier as an enlarged *trans*-Golgi compartment [23,28]. The same structures were also found to recruit GFP-Lact-C2, implying that PS is exposed on the cytosolic leaflet of these membranes. More importantly, by blocking secretion the *sec7* mutation prevented the accumulation of PS at budding sites, in agreement with the preceding results. Jointly, these findings suggest that targeted secretion of PS-enriched vesicles underlies the polarization of the phospholipid in budding yeast.

Retrieval of PS from endosomes

Polarized secretion at budding sites is accompanied by elevated rates of endocytosis [29,30]. For a gradient of PS to be maintained, the phospholipid must therefore be preferentially excluded from forming endosomes or effectively recycled back to sites of polarized exocytosis. We used two different mutants to analyze if endosomes formed during vegetative growth contain PS and whether their recycling to the surface membrane is required to establish and maintain the accumulation of PS at the bud. Sec14 was recently shown to be required for recycling of Snc1 to the plasma membrane and for transport of a membrane marker, FM4-64, through the endocytic pathway [31,32]. We co-transformed the temperature-sensitive mutant *sec14^{ts}* cells with mRFP-Snc1 and GFP-Lact-C2 and compared the pattern of expression of these probes at the permissive and restrictive temperatures. At 25ºC mRFP-Snc1 was localized almost exclusively to the bud and GFP-Lact-C2 showed a similar distribution (Fig. 3a). After 60 min at 37ºC, however, both probes relocalized to internal structures likely to be endosomal in nature. Of note, the concentration of GFP-Lact-C2 at the bud was considerably attenuated, suggesting that normal retrieval of PS from endosomes is required for PS accumulation.

In addition to its role in endocytosis, Sec14 is required for proper vesicle generation at the *trans*-Golgi [33,34]. Because secretory vesicles were shown earlier to be endowed with PS, it was conceivable that the PS-enriched structures formed in *sec14^{ts}* cells represented an enlarged *trans*-Golgi, rather than endosomes. This possibility was assessed by comparing the distribution of GFP-Lact-C2 and of Sec7-RFP*,* a *trans*-Golgi resident protein. As illustrated in Fig. 3b, the appearance of Sec7-RFP was not grossly altered by transferring the mutant cells to 37ºC and, importantly, the *trans*-Golgi marker did not co-localize with the GFP-Lact-C2-containing structures, suggesting that the latter are indeed of endosomal origin.

To more unambiguously establish the requirement for retrieval from endosomes we also examined cells lacking Rcy1. Rcy1, an atypical F-box protein, is required for the efflux of FM4-64 from endosomes and for the retrieval of Snc1 from early endosomes to the Golgi [35,36]. In

*rcy1*Δ cells, GFP-Lact-C2 co-localizes with mRFP-Snc1 in internal structures (Fig. 3c), confirming their identity as endosomes. As in the case of *sec14*^{ts} cells, the accumulation of GFP-Lact-C2 in the limiting membrane of buds was attenuated, but not eliminated. Jointly, these findings suggest that while concentrated PS is delivered to the bud membrane by the secretory pathway, at least a fraction of the PS is internalized by endocytosis and normal recycling of PS-enriched vesicles is required for the maintenance of the concentration gradient at the bud.

Diffusion rate of inner leaflet phospholipids in yeast

Membrane lipids are capable of diffusing in the plane of the bilayer. For a steady gradient of PS to be maintained between the bud and the bulk membrane of the mother cell, the rate of delivery of the phospholipid to the bud must exceed the rate of lateral diffusion. In this regard, it is noteworthy that the rates of diffusion of tagged lipids (e.g. rhodamine-phosphatidylethanolamine) and of lipophilic probes (e.g. DiI) along the exofacial leaflet of the yeast plasma membrane are comparatively slow, approximately 10-fold lower than those reported in mammalian cells [37]. Similarly, Snc1 and another yeast SNARE protein, Sso1, diffuse ≈40-fold more slowly when expressed in the membrane of yeast than in mammalian membranes [9]. The slow diffusion of yeast plasmalemmal components could, in principle, contribute to the maintenance of PS polarization in budding yeast. However, the reduced mobility of exofacial and transmembrane components has been attributed to the presence of ergosterol and/or to interactions with the cell wall [9], which may not affect lipids of the inner leaflet. Because no such determinations were available, we measured the rate of diffusion of lipid-associated probes that partition to the cytosolic monolayer of the yeast plasma membrane. We measured the rate of GFP-Lact-C2 fluorescence recovery after photobleaching (FRAP) to determine the mobility of PS in the inner leaflet. When a spot of 2 μm diameter was bleached (Fig. 4a), fluorescence recovery was half-maximal after 35.1 ± 2.2 sec (Fig. 4b), which

corresponds to a diffusion coefficient of 0.007 μm^2/sec. This value is markedly slower than the coefficients reported for phospholipids in mammalian cell membranes, which typically range from 0.3 - 0.4 μm^2/sec [38].

Because the GFP-Lact-C2 probe is reversible, the recovery from photobleaching may have been influenced by dissociation and reassociation of the probe, in addition to lateral diffusion. The relative contribution of these two components was probed by analyzing the shape of the photobleaching pattern as a function of time. The optical features of our illumination system used yielded a Gaussian photobleaching pattern (Fig. 4d). A widening of the Gaussian curve over time would be anticipated if lateral motion of the lipid/probe complex contributes significantly to the fluorescence recovery process. Conversely, failure of the Gaussian pattern to widen would indicate that probe dissociation and reassociation is the predominant mechanism (see Oancea et al., 1998 for details). As shown in Fig. 4d, the curve widened during the course of the recovery, implying that probe dissociation was comparatively slow and that lateral diffusion was a sizable component of the measured rate of recovery.

To validate this conclusion we compared the rate of diffusion calculated for PS using GFP-Lact-C2 with that of a different probe that is retained in the membrane by hydrophobic interactions. To this end we used a palmitoylated and farnesylated form of GFP, generated by attachment of the C-terminal region (a.a. 288-322) of the yeast Ras2 protein. The resulting acylated chimera, named GFP-RT, partitions selectively into the inner leaflet of the yeast plasma membrane (Fig. 4b) and can be used as a surrogate to measure lipid mobility. Of note, the diffusion coefficient of soluble GFP is orders of magnitude greater than that of the membrane-associated chimera [39], implying that the lateral displacement of the lipid tails is the step that limits its rate of diffusion in the membrane. Using the same FRAP protocol described above, we calculated a diffusion coefficient of 0.012 μm^2/sec for GFT-RT in the buds. This value is of the same order as that calculated for GFP-Lact-C2, and is similarly much slower than

the values reported for lipids or lipid-associated probes in mammalian membranes. Together, these results suggest that PS, like DiI and rhodamine-PE and possibly other lipids, diffuse slowly in the inner leaflet of the yeast PM. This slow rate of diffusion likely contributes to the generation and maintenance of PS polarization at sites of bud emergence.

Growth and polarization defects in cells lacking PS

We next examined whether the polarization of PS observed during budding is required for optimal cell growth. The growth rate of yeast lacking PS was compared to that of the isogenic wild-type cells. In *S. cerevisiae* a single synthase is responsible for the biosynthesis of PS. Cells lacking the gene encoding the PS-synthase, referred to as *cho1*Δ/*pss1*Δ [40], grew considerably slower than the parental strain on rich agar medium, implying that PS is important for optimal growth (Fig. 5a) [41]. However, compensatory changes in the lipid profile enable most functions in *cho1*Δ cells to proceed normally, to the extent that FM4-64 uptake, α-factor maturation, CPY trafficking and localization of the septin ring are unaltered ([42,43] and our published observations). As shown above (Fig. 1), the first instance when PS is seen to polarize during the cell cycle coincides with bud emergence. This is also the time when the cellular PS content is highest [13]. We therefore hypothesized that the initial establishment of polarized exocytosis delivers PS via secretory vesicles to the incipient bud site and that delivery of PS may be required to support optimal bud growth. This hypothesis predicts that *cho1*Δ cells may have a delay in bud emergence/formation. Cell cycle synchronization was used to examine the time required for bud emergence in 1607-5D wild-type cells and in an isogenic *cho1::kanMX* strain. Large unbudded cells accumulated when growth was arrested in late G1 phase of the cycle by glucose-induced depletion of the G1 cyclin Cln3 in *cln1*Δ*, cln2*Δ*, pGAL-CLN3* cells [44]. Release from G1 arrest was accomplished by replacement of glucose with galactose, and aliquots of cells were then removed at 60 min intervals and fixed with 4%

formaldehyde for subsequent microscopic examination. Sixty min after galactose induction ≈30% of the wild-type cells had buds, and this number increased to ≈80% after 120 min. In contrast, only ≈2% of the *cho1*Δ cells had buds after 60 min, while ≈10% did so after 120 min and ≈25% after 180 min (Fig. 5b). The results are consistent with the notion that PS, and likely its polarization at sites of bud formation, are functionally important to support cell polarity and bud emergence.

Bud formation in yeast requires the small GTPase Cdc42 [45]. Cdc42 has been shown to cluster at the site of bud emergence and to reside on vesicles in close proximity to the bud [2,46], resembling the pattern of PS polarization described above. We therefore wondered if clustering of Cdc42 requires PS. Parental and *cho1*Δ cells expressing a GFP-Cdc42 construct under control of the *MET25* promoter were grown in medium containing 400 μM methionine, to partly repress GFP-Cdc42 expression, as the parental and *cho1*Δ cells have an untagged genomic copy of *CDC42* [47]. In agreement with previous reports [46], in wild-type yeast GFP-Cdc42 was found to be enriched in the plasma membrane at sites of bud emergence and in the bud cortex of small-budded cells (Fig. 5c), although GFP-Cdc42 could also be detected throughout the plasma membrane and on other organelles. In the *cho1*Δ cells, in contrast, GFP-Cdc42 was not visibly enriched at the sites of bud emergence or in small buds and there was an overall decrease in plasmalemmal binding. Instead, the amount of GFP-Cdc42 associated with internal organelles increased (Fig. 5c). These results demonstrate that PS is required for proper localization of Cdc42 to the plasma membrane and for its clustering during bud formation. The altered localization of Cdc42 correlates with, and is most likely responsible for the impaired bud emergence and cell growth of the PS-deficient mutants.

Under normal circumstances, the enrichment of Cdc42 at sites of polarization relies on a positive feedback loop: a) Cdc24 activates Cdc42 through GTP-loading; b) GTP-Cdc42 in turn recruits the adaptor protein, Bem1 and c) Bem1 interacts physically with Cdc24, generating a

tripartite cluster of Cdc42, Cdc24, and Bem1 [3]. The abundance of PS in the plasmalemma and its enrichment at sites of polarized growth suggest that the PS-rich membrane may serve as a scaffold that recruits and/or supports the activity of the Cdc42 signaling complex. To further examine the role of PS in Cdc42-complex signaling, wild-type and *cho1Δ* cells were transformed with a plasmid expressing Bem1-GFP. As seen in Fig. 5d, in wild-type cells Bem1-GFP localized to the site of bud emergence and to the tips of buds. As was the case for GFP-Cdc42, the polarization of Bem1-GFP to sites of bud emergence or bud tips was greatly reduced in *cho1Δ* cells (Fig. 5d). These results indicate that the absence of PS reduced not only the total amount of Cdc42 at the bud, but that there are in fact fewer active Cdc42-signaling complexes at this site.

Mating defects in cells lacking PS

To further investigate the importance of PS in cell polarity, we next examined whether the phospholipid is required to support another well-characterized polarization process that depends on Cdc42, namely mating. Stimulation of the G protein-coupled receptor Ste2 by mating factor α leads to the activation of the $G\beta\gamma$ subunits [48]. At sites of receptor-ligand association the $G\beta\gamma$ subunits recruit Far1, which in turn recruits Cdc24, leading to Cdc42 activation [49,50]. As during bud formation, Cdc42 activation generates a polarity axis leading to the directed secretion of vesicles to the tips of the mating projections. Because polarization of PS in the buds of yeast is the result of vectorial secretion, we analyzed whether PS also becomes polarized in cells exposed to mating factor. Fig. 6a shows images of wild-type cells expressing GFP-Lact-C2 that were exposed to 5 μM mating factor α for 3 h. When compared to the rest of the plasma membrane, the mating projections were clearly enriched in PS. As in the case of the vegetative yeast, we used other membrane probes to rule out optical or membrane density artifacts. Both the PH domain of PLCδ, a probe for $PI4,5P_2$, (Fig. 6b), and GFP-Ras2

(Fig. 6c) distributed evenly throughout the plasma membrane, without concentrating in the mating projections. To verify that GFP-Lact-C2 accumulation reflects polarization of PS in the shmoo, the probe was expressed in *cho1*Δ cells that were then exposed to mating factor. As shown in Fig. 6a, GFP-Lact-C2 was largely soluble in the mutant cells, confirming earlier results [14] and implying that PS is indeed accumulated in mating projections.

Because PS is required for optimal Cdc42 function in vegetative cells and this GTPase is required for the formation of mating projections, we considered whether cells lacking PS might have impaired ability to mate. This hypothesis was lent further credence by the observation that *cho1*Δ cells failed to make proper mating projections when stimulated by mating factor (e.g. Fig. 6a). As shown in Fig. 6c, when *cho1Δ* cells were crossed with a 10-fold excess of *CHO1* cells the mating efficiency was only 5%, compared to nearly 100% for the wild-type counterparts. We next examined whether impaired Cdc42 signaling was responsible for the inability of the PS-deficient cells to mate. Wild-type and *cho1Δ* cells were transformed with pMET-GFP-Cdc42, grown to mid-log phase and treated with mating factor α for 3 h in the presence of 400 μM to allow for partial expression. In wild-type cells, GFP-Cdc42 was found enriched at the tip of the mating projection compared to the rest of the plasma membrane (Fig. 6d), as reported earlier (Ziman et al., 1993; [51]. The *cho1Δ* cells expressing GFP-Cdc42 had atypical morphology, often having either a peanut shape or forming multiple projections (Fig. 6d). Regardless of their shape, however, little enrichment of GFP-Cdc42 was seen at the tips of the projections in the *cho1Δ* cells.

Previous reports demonstrated that Cdc24, like Cdc42, is localized to the tips of mating projections in wild-type cells [3]. These observations were confirmed in Fig. 6e using GFP-Cdc24, which also accumulated in the nucleus. In *cho1Δ* cells GFP-Cdc24 showed very modest association with the plasma membrane and a strong presence in the nucleus. The mislocalization of GFP-Cdc42 and GFP-Cdc24 in *cho1Δ* cells suggests that the level of active

(GTP-bound) Cdc42 may be diminished in their projections. This was examined further in cells transformed with an integrating plasmid encoding a reporter of GTP-bound Cdc42, namely the Gic2 p21-binding domain (PBD) fused to RFP [52]. Gic2-PBD-RFP was localized to the tips of mating projections in wild-type cells (Fig. 6f). It should be noted that cells expressing Gic2-PDB-RFP and treated with mating factor have an abnormal shape compared to untransfected cells (*cf.* Fig. 6a and f), implying that the fluorescent reporter is not entirely inert. In the *cho1Δ* cells the Gic2-PBD-RFP is localized to several areas of the plasma membrane, not necessarily corresponding to projections. Importantly, more cytosolic Gic2-PBD-RFP signal is present in the PS-deficient mutants, suggesting that they contain less GTP-bound Cdc42.

Taken together, the preceding results demonstrate that Cdc42 localization and activation are impaired in cells lacking PS. The presence of a fraction of membrane-associated Gic2-PBD-RFP implies that Cdc42 can be partially activated by Cdc24, but suggests that GTP-Cdc42 fails to assemble into normal complexes with its effector proteins. In particular, it appeared likely that the association of Cdc42 with Bem1 was impaired, since Bem1 not only stabilizes the Cdc42/Cdc24 complex, but is known to localize to the tip of the mating projections [3]. We verified the localization of Bem1 to the tips of shmoos in wild-type cells (Fig. 6g) and analyzed its distribution in *cho1Δ* cells also. As shown in Fig. 6g, Bem1-GFP was not enriched in the plasma membrane of the PS-deficient cells. These findings suggest that PS, and likely its polarization, are required for proper formation of projections and mating.

Role of electrostatic interactions in Cdc42 signaling

We next analyzed the mechanism whereby lipids contribute to direct Cdc42 to defined regions of the membrane. The GTPase itself, as well as several of its associated proteins, possess lipid-interacting motifs or domains. As illustrated in Fig. 7a, several members of the Cdc42 complex display polycationic motifs that are known or anticipated to associate

electrostatically with negatively-charged surfaces [53,54]. Others contain PH or PX domains that bind to PS or to phosphoinositides, particularly PI4P [55,56].

We therefore examined the distribution of PI4P using the PH domain of Osh2 [57]. In wild-type yeast, this probe was found to concentrate in the bud membrane and in neighboring submembranous vesicles and/or compartments (Fig. 7b). Remarkably, the distribution of GFP-PH-Osh2 was very similar in *cho1Δ* cells (Fig. 7b). This finding implies that PS is not required for polarization of PI4P and, more importantly, that this phosphoinositide is most likely not responsible for the accumulation of Cdc42-complex proteins at the bud, which is defective in *cho1Δ* cells.

PS is the most abundant phospholipid of the plasma membrane, where it is largely confined to the inner leaflet [11,12]. The abundance and asymmetric distribution of PS, together with its anionic nature, confer to the cytosolic monolayer a sizable anionic surface charge. The uniquely elevated concentration of PS at budding sites and in mating projections would accentuate this charge further, favoring the local association with polycationic peptides and proteins. This prediction was validated using a recently developed probe of surface charge [58]. The GFP+8 probe, a coincidence detector consisting of a polybasic motif in the vicinity of a hydrophobic (prenyl) moiety, partitioned largely to the inner leaflet of the yeast plasma membrane (Fig. 7c), implying that it is the most negatively-charged surface of the cell. As predicted, the surface charge was highest at the bud, likely because of the localized accumulation of PS and PI4P. In *cho1Δ* cells a smaller fraction of the GFP+8 probe was found at the surface membrane (Fig. 7c). Instead, much of the probe was associated with endomembrane structures. Of note, the preferential accumulation of GFP+8 seen in the buds of wild-type yeast was absent in *cho1Δ* cells, implying that PS is required for the polarization of anionic charge in the membrane. The differences in the distribution of GFP+8 in wild-type and

cho1Δ cells are reminiscent of those seen for Cdc42 in Fig. 5, suggesting that surface charge may contribute significantly to the targeting of the GTPase complex.

DISCUSSION

Lipids as spatial regulators of polarity

In mammalian cells, phospholipids play a central role in the establishment of cell polarity**.** The polarized generation of phosphatidylinositol 3,4,5-*tris*phosphate (PI3,4,5P_3) from PI4,5P_2 is key to chemotaxis, macropinocytosis and other vectorial processes. Yeast, however, lack the class I phosphatidylinositol 3-kinases that generate PI3,4,5P_3 in animal cells. Other spatial cues are therefore necessary for yeast to establish and maintain polarity during budding and mating, and alternative lipids could be of importance. Our results suggest that PS can serve this function in *S. cerevisiae*. Using a recently developed genetically-encoded fluorescent probe, in combination with PS synthase-deficient mutants, we demonstrated that PS polarizes and is required for proper budding and mating. The underlying mechanisms and implications of this polarization are discussed below.

Mechanisms of PS polarization

The distribution of lipids, including PS, varies greatly between organelles. The plasma membrane is the predominant reservoir of several lipids including PS, ergosterol and sphingolipids. Accumulation of ergosterol and sphingolipids at the membrane results from preferential delivery of these lipids by the secretory pathway, and a similar mechanism likely accounts for the plasmalemmal enrichment of PS. Accordingly, PS-rich vesicles accumulated in Sec1, and Sec6 -deficient mutants, with corresponding depletion of plasmalemmal PS.

At least two processes can be envisaged to contribute to the selective enrichment of PS in secretory vesicles: i) partition into ergosterol- and sphingolipid-rich lipid microdomains (“rafts”) or ii) transmembrane flipping-induced segregation. Recent yeast lipidomics studies revealed that the plasmalemmal PS has an elevated content of saturated acyl chains [59]. Highly saturated PS may spontaneously segregate into the ergosterol and sphingolipid-enriched secretory vesicles known to be generated in the Golgi complex [60]. This possibility, however, is not

supported by the recent report that low-density secretory vesicles (LDSV), though enriched in raft-inducing lipids, are largely deficient in PS and PE [60]. Alternatively, PS may accumulate in the high-density secretory vesicles (HDSV), which are clathrin-coated, by a different mechanism. The phospholipid translocase Drs2, which is found primarily in the yeast *trans*-Golgi, displays a preference for PS over other phospholipids [61]. Translocase activity can drive membrane bending towards the cytosol by increasing the number of phospholipids in the cytosolic leaflet compared to the luminal leaflet. If, as proposed [62], this curvature facilitates membrane evagination and scission, the resulting secretory vesicles would be naturally enriched in PS. Because components of the clathrin assembly machinery preferentially bind to anionic lipids [63,64], sites of active PS flipping would have both the curvature and charge to promote clathrin-mediated vesiculation. The resulting HDSV would deliver their PS-enriched bilayer to the plasmalemma.

Regardless of whether HDSV or LDSV are responsible for selectively delivering PS to the plasma membrane, a similar process appeared likely to account for PS enrichment at budding and mating processes. This prediction is supported by the observation that PS polarization in the membrane of budding yeast was virtually eliminated by mutations that arrest the secretory pathway at either intermediate (Sec7) or late (Sec1 and Sec6) stages (Fig. 2). It is noteworthy that sterols and sphingolipids, which are also segregated in the Golgi complex, were recently reported to accumulate in mating projections [8]. This raises the possibility that PS may secondarily partition into microdomains at the plasma membrane and that the effects of inhibiting secretion are indirect. However, in the secretion-defective mutants the dissipation of the PS concentration gradient in the bud membrane was accompanied by the appearance of PS-endowed endomembrane vesicles. This implies that the phospholipid is concentrated along the secretory pathway en route to the plasma membrane, rather than becoming retained at the surface membrane by rafts.

Endocytosis, which is active at sites of budding and at mating projections, is expected to counteract the accumulation of PS at sites of polarization. The material that reaches endosomes can undergo three different fates: recycling to the membrane, retrograde traffic to the Golgi complex and delivery to the prevacuolar compartment and ultimately to the vacuole. Both direct biochemical analysis [11], as well as analysis of the distribution of the GFP-Lact-C2 probe (e.g. Figs. 1-2) indicate that the PS content of the vacuole is markedly lower than that of the plasma membrane. This implies that PS is either segregated and redirected to another compartment en route to the vacuole and/or degraded therein. The notion that PS is segregated and recycled to the membrane is lent credence by observations made in *sec14*^{ts} and *rcy1*Δ cells. In both mutants PS co-segregated in internal vesicles with Snc1, an integral membrane protein known to recycle actively [9,23]. The concomitant attenuation of PS accumulation in the buds of the mutant cells suggests that continued recycling of PS is required for optimal establishment of its gradient at sites of polarization. Thus, vectorial secretion and recycling combine to maintain a uniquely elevated concentration of PS in buds and mating projections.

For a PS gradient to be sustained at buds and mating projections, the rate of vesicular delivery must exceed the tendency of the lipid to diffuse in the plane of the membrane. The existence of a diffusional barrier at the neck could conceivably explain the retention of lipids in the bud. Indeed, the septins that ring the bud neck have been reported to limit the diffusion of proteins [65]. However, no such structure is observed in mating projections, where PS accumulation was readily noticeable. On the other hand, FRAP determinations indicated that PS, as well as other lipid molecules in the inner leaflet, diffuse remarkably slowly. The slow diffusion rates of PS were not unique to the bud (not shown), suggesting that they are a general feature of the yeast surface membrane. Accordingly, the lateral translation rates of yeast exofacial lipids or transmembrane proteins were earlier found to be up to 40-fold slower than those reported in mammalian membranes [9,37]. Whether the presence of ergosterol or

interactions with the rigid cell wall are responsible for this behavior remains undefined. Regardless of the mechanism, however, it is most likely that the slow rate of lipid diffusion contributes to the generation and maintenance of PS polarization at sites where buds and mating projections emerge.

Polarization of PS supports a positive feedback loop for Cdc42 activation.

The localized accumulation of GTP-Cdc42 is central to the establishment of a directional axis during bud emergence and formation of mating projections. A positive feedback loop has been proposed to drive polarization: when activated by Cdc24, Cdc42 binds to its effector, Bem1, which in turns recruits additional Cdc24. All three of these proteins, as well as a number of other Cdc42-associated proteins, possess membrane-targeting determinants, notably polybasic motifs or domains that preferentially bind anionic phospholipids [46,53,54,56,66]. While in some instances PI4P is preferred, binding to PS is likely to be the predominant factor in targeting most proteins: its large concentration in the membrane (estimated to reach 50-60 mol % in the inner leaflet, compared to only 1-2% PI4P) is likely to outweigh the differential affinity. In the absence of PS other negatively charged lipids, likely phosphoinositides, may provide sufficient signal to maintain viability; however this does not appear sufficient to support robust growth or mating.

Two mechanisms can be envisaged to drive the accumulation of Cdc42-complex proteins at buds and in mating projections: PS could be stereospecifically recognized by three-dimensional domains like the Phox homology domain of Bem1 or the partial Pleckstrin homology domain of Cdc24. Alternatively, the interaction may be predominantly electrostatic; the development of a surface charge gradient, more negative in the bud than in the mother cell membrane (Fig. 7), is consistent with this concept. In either case, other targeting determinants including protein-protein interactions are likely to exist, as it is becoming increasingly obvious that most, if not all proteins are targeted to membranes by the simultaneous recognition of multiple individual

determinants, which are necessary but by themselves insufficient for accurate recruitment. Accumulation of PS at the bud or mating projection, however, is clearly necessary for optimal targeting and function of the Cdc42 complex in establishing cell polarity.

EXPERIMENTAL PROCEDURES

Yeast strains used are listed in the Supplemental Data section. Standard media and methods were used for plasmid and yeast molecular manipulations. Further information is included in the supplemental experimental procedures.

Mating assay

For quantitative mating assays, cells were grown to mid-log phase in YPD medium and then 10^6 **a** cells were mixed with 10^7 α partner cells and collected into a soft pellet by centrifugation. After 4 h of mating at 30°C, cells were suspended in liquid and serial dilutions were plated on medium selective for diploids. Mating efficiency was calculated as the percentage of input **a** cells that formed diploids; the number of input cells was determined by plating a dilution of the **a** cell cultures on selective or complete plates at the start of the mating assay. The mating efficiency for parental BY4741 cells was >95%. The assay was performed 3 times with > 2000 cells examined per condition.

Fluorescence microscopy

All fluorescence images were acquired using spinning-disc confocal microscopy. The systems used (Quorum) are based on a Zeiss Axiovert 200M microscope with 100X objective. The units are equipped with diode-pumped solid-state laser lines (440 nm, 491 nm, 561 nm, 638 nm, 655 nm; Spectral Applied Research), motorized XY stage (ASI) and piezo focus drive. Images were acquired using either back-thinned, electron-multiplied or conventional cooled charge-coupled device cameras (Hamamatsu), driven by the Volocity 4.1.1 software (Improvision).

Imaging of Cells

Cells were grown to early log phase, harvested by centrifugation, washed with PBS or resuspended in fresh medium. Mating projections were formed by incubating cells with 5 μM

mating factor α for ≈3 h. Cells were attached to coverslips treated with concanavalin A or mounted on agarose pads.

For FRAP experiments, cells were resuspended in growth medium, spotted on medium containing agarose pads, and covered with glass coverslips. Cells were imaged with a 100X objective and a bleaching area defined, as indicated. The fluorescence intensities of the bleached area were determined at various time points and corrected for photobleaching incurred during image acquisition by dividing by the total cell fluorescence at the corresponding time point.

ACKNOWLEDGMENTS

We thank Drs. Chris McMaster, Scott Emr, Hugh Pelham, Tim Levine, Douglas Johnson, Kazuma Tanaka, Ruth Collins, Erfei Bi, Rong Li, Fred Cross and Charlie Boone for strains and plasmids. We also thank Dr. C. McMaster for his comments on the manuscript. This work was supported by Canadian Institutes of Health Research (CIHR) grants 7075 and MOP4665. G. D. F. is the recipient of a CIHR postdoctoral fellowship. S.G. is the current holder of the Pitblado Chair in Cell Biology.

REFERENCES

1. Etienne-Manneville, S. & Hall, A. Rho GTPases in cell biology. *Nature* **420**, 629-35 (2002).

2. Ziman, M. et al. Subcellular localization of Cdc42p, a Saccharomyces cerevisiae GTP-binding protein involved in the control of cell polarity. *Mol Biol Cell* **4**, 1307-16 (1993).

3. Butty, A.C. et al. A positive feedback loop stabilizes the guanine-nucleotide exchange factor Cdc24 at sites of polarization. *Embo J* **21**, 1565-76 (2002).

4. Johnson, D.I. Cdc42: An essential Rho-type GTPase controlling eukaryotic cell polarity. *Microbiol Mol Biol Rev* **63**, 54-105 (1999).

5. Kozubowski, L. et al. Symmetry-breaking polarization driven by a Cdc42p GEF-PAK complex. *Curr Biol* **18**, 1719-26 (2008).

6. Irazoqui, J.E., Gladfelter, A.S. & Lew, D.J. Scaffold-mediated symmetry breaking by Cdc42p. *Nat Cell Biol* **5**, 1062-70 (2003).

7. Wedlich-Soldner, R., Altschuler, S., Wu, L. & Li, R. Spontaneous cell polarization through actomyosin-based delivery of the Cdc42 GTPase. *Science* **299**, 1231-5 (2003).

8. Proszynski, T.J., Klemm, R., Bagnat, M., Gaus, K. & Simons, K. Plasma membrane polarization during mating in yeast cells. *J Cell Biol* **173**, 861-6 (2006).

9. Valdez-Taubas, J. & Pelham, H.R. Slow diffusion of proteins in the yeast plasma membrane allows polarity to be maintained by endocytic cycling. *Curr Biol* **13**, 1636-40 (2003).

10. Vance, J.E. Phosphatidylserine and phosphatidylethanolamine in mammalian cells: two metabolically related aminophospholipids. *J Lipid Res* **49**, 1377-87 (2008).

11. Zinser, E. et al. Phospholipid synthesis and lipid composition of subcellular membranes in the unicellular eukaryote Saccharomyces cerevisiae. *J Bacteriol* **173**, 2026-34 (1991).

12. van Meer, G., Voelker, D.R. & Feigenson, G.W. Membrane lipids: where they are and how they behave. *Nat Rev Mol Cell Biol* **9**, 112-24 (2008).

13. Cottrell, S.F., Getz, G.S. & Rabinowitz, M. Phospholipid accumulation during the cell cycle in synchronous cultures of the yeast, Saccharomyces cerevisiae. *J Biol Chem* **256**, 10973-8 (1981).

14. Yeung, T. et al. Membrane phosphatidylserine regulates surface charge and protein localization. *Science* **319**, 210-3 (2008).

15. Jin, H., McCaffery, J.M. & Grote, E. Ergosterol promotes pheromone signaling and plasma membrane fusion in mating yeast. *J Cell Biol* **180**, 813-26 (2008).

16. Fujiyama, A., Tsunasawa, S., Tamanoi, F. & Sakiyama, F. S-farnesylation and methyl esterification of C-terminal domain of yeast RAS2 protein prior to fatty acid acylation. *J Biol Chem* **266**, 17926-31 (1991).

17. Norden, C. et al. The NoCut pathway links completion of cytokinesis to spindle midzone function to prevent chromosome breakage. *Cell* **125**, 85-98 (2006).

18. Trotter, P.J. & Voelker, D.R. Identification of a non-mitochondrial phosphatidylserine decarboxylase activity (PSD2) in the yeast Saccharomyces cerevisiae. *J Biol Chem* **270**, 6062-70 (1995).

19. Finger, F.P., Hughes, T.E. & Novick, P. Sec3p is a spatial landmark for polarized secretion in budding yeast. *Cell* **92**, 559-71 (1998).

20. Finger, F.P. & Novick, P. Spatial regulation of exocytosis: lessons from yeast. *J Cell Biol* **142**, 609-12 (1998).

21. Schekman, R. & Novick, P. 23 genes, 23 years later. *Cell* **116**, S13-5, 1 p following S19 (2004).

22. Gurunathan, S., David, D. & Gerst, J.E. Dynamin and clathrin are required for the biogenesis of a distinct class of secretory vesicles in yeast. *Embo J* **21**, 602-14 (2002).

23. Lewis, M.J., Nichols, B.J., Prescianotto-Baschong, C., Riezman, H. & Pelham, H.R. Specific retrieval of the exocytic SNARE Snc1p from early yeast endosomes. *Mol Biol Cell* **11**, 23-38 (2000).

24. Harsay, E. & Schekman, R. A subset of yeast vacuolar protein sorting mutants is blocked in one branch of the exocytic pathway. *J Cell Biol* **156**, 271-85 (2002).

25. Achstetter, T., Franzusoff, A., Field, C. & Schekman, R. SEC7 encodes an unusual, high molecular weight protein required for membrane traffic from the yeast Golgi apparatus. *J Biol Chem* **263**, 11711-7 (1988).

26. Chardin, P. et al. A human exchange factor for ARF contains Sec7- and pleckstrin-homology domains. *Nature* **384**, 481-4 (1996).

27. Sata, M., Donaldson, J.G., Moss, J. & Vaughan, M. Brefeldin A-inhibited guanine nucleotide-exchange activity of Sec7 domain from yeast Sec7 with yeast and mammalian ADP ribosylation factors. *Proc Natl Acad Sci U S A* **95**, 4204-8 (1998).

28. Novick, P., Field, C. & Schekman, R. Identification of 23 complementation groups required for post-translational events in the yeast secretory pathway. *Cell* **21**, 205-15 (1980).

29. Irazoqui, J.E., Howell, A.S., Theesfeld, C.L. & Lew, D.J. Opposing roles for actin in Cdc42p polarization. *Mol Biol Cell* **16**, 1296-304 (2005).

30. Kaksonen, M., Sun, Y. & Drubin, D.G. A pathway for association of receptors, adaptors, and actin during endocytic internalization. *Cell* **115**, 475-87 (2003).

31. Curwin, A.J., Fairn, G.D. & McMaster, C.R. Phospholipid transfer protein Sec14 is required for trafficking from endosomes and regulates distinct trans-Golgi export pathways. *J Biol Chem* **284**, 7364-75 (2009).

32. Mousley, C.J. et al. Trans-Golgi network and endosome dynamics connect ceramide homeostasis with regulation of the unfolded protein response and TOR signaling in yeast. *Mol Biol Cell* **19**, 4785-803 (2008).

33. Bankaitis, V.A., Malehorn, D.E., Emr, S.D. & Greene, R. The Saccharomyces cerevisiae SEC14 gene encodes a cytosolic factor that is required for transport of secretory proteins from the yeast Golgi complex. *J Cell Biol* **108**, 1271-81 (1989).

34. Bankaitis, V.A., Aitken, J.R., Cleves, A.E. & Dowhan, W. An essential role for a phospholipid transfer protein in yeast Golgi function. *Nature* **347**, 561-2 (1990).

35. Bensen, E.S., Yeung, B.G. & Payne, G.S. Ric1p and the Ypt6p GTPase function in a common pathway required for localization of trans-Golgi network membrane proteins. *Mol Biol Cell* **12**, 13-26 (2001).

36. Wiederkehr, A., Avaro, S., Prescianotto-Baschong, C., Haguenauer-Tsapis, R. & Riezman, H. The F-box protein Rcy1p is involved in endocytic membrane traffic and recycling out of an early endosome in Saccharomyces cerevisiae. *J Cell Biol* **149**, 397-410 (2000).

37. Greenberg, M.L. & Axelrod, D. Anomalously slow mobility of fluorescent lipid probes in the plasma membrane of the yeast Saccharomyces cerevisiae. *J Membr Biol* **131**, 115-27 (1993).

38. Murase, K. et al. Ultrafine membrane compartments for molecular diffusion as revealed by single molecule techniques. *Biophys J* **86**, 4075-93 (2004).

39. Swaminathan, R., Bicknese, S., Periasamy, N. & Verkman, A.S. Cytoplasmic viscosity near the cell plasma membrane: translational diffusion of a small fluorescent solute measured by total internal reflection-fluorescence photobleaching recovery. *Biophys J* **71**, 1140-51 (1996).

40. Atkinson, K.D. et al. Yeast mutants auxotrophic for choline or ethanolamine. *J Bacteriol* **141**, 558-64 (1980).

41. Atkinson, K., Fogel, S. & Henry, S.A. Yeast mutant defective in phosphatidylserine synthesis. *J Biol Chem* **255**, 6653-61 (1980).

42. Natarajan, P., Wang, J., Hua, Z. & Graham, T.R. Drs2p-coupled aminophospholipid translocase activity in yeast Golgi membranes and relationship to in vivo function. *Proc Natl Acad Sci U S A* **101**, 10614-9 (2004).

43. Yeung, T. et al. Contribution of phosphatidylserine to membrane surface charge and protein targeting during phagosome maturation. *J Cell Biol* **185**, 917-28 (2009).

44. Cross, F.R. Cell cycle arrest caused by CLN gene deficiency in Saccharomyces cerevisiae resembles START-I arrest and is independent of the mating-pheromone signalling pathway. *Mol Cell Biol* **10**, 6482-90 (1990).

45. Johnson, D.I. & Pringle, J.R. Molecular characterization of CDC42, a Saccharomyces cerevisiae gene involved in the development of cell polarity. *J Cell Biol* **111**, 143-52 (1990).

46. Richman, T.J., Sawyer, M.M. & Johnson, D.I. Saccharomyces cerevisiae Cdc42p localizes to cellular membranes and clusters at sites of polarized growth. *Eukaryot Cell* **1**, 458-68 (2002).

47. Mumberg, D., Muller, R. & Funk, M. Regulatable promoters of Saccharomyces cerevisiae: comparison of transcriptional activity and their use for heterologous expression. *Nucleic Acids Res* **22**, 5767-8 (1994).

48. Whiteway, M. et al. The STE4 and STE18 genes of yeast encode potential beta and gamma subunits of the mating factor receptor-coupled G protein. *Cell* **56**, 467-77 (1989).

49. Zhao, Z.S., Leung, T., Manser, E. & Lim, L. Pheromone signalling in Saccharomyces cerevisiae requires the small GTP-binding protein Cdc42p and its activator CDC24. *Mol Cell Biol* **15**, 5246-57 (1995).

50. Wiget, P., Shimada, Y., Butty, A.C., Bi, E. & Peter, M. Site-specific regulation of the GEF Cdc24p by the scaffold protein Far1p during yeast mating. *Embo J* **23**, 1063-74 (2004).

51. Barale, S., McCusker, D. & Arkowitz, R.A. Cdc42p GDP/GTP cycling is necessary for efficient cell fusion during yeast mating. *Mol Biol Cell* **17**, 2824-38 (2006).

52. Tong, Z. et al. Adjacent positioning of cellular structures enabled by a Cdc42 GTPase-activating protein-mediated zone of inhibition. *J Cell Biol* **179**, 1375-84 (2007).

53. Takahashi, S. & Pryciak, P.M. Identification of novel membrane-binding domains in multiple yeast Cdc42 effectors. *Mol Biol Cell* **18**, 4945-56 (2007).

54. Winters, M.J., Lamson, R.E., Nakanishi, H., Neiman, A.M. & Pryciak, P.M. A membrane binding domain in the ste5 scaffold synergizes with gbetagamma binding to control localization and signaling in pheromone response. *Mol Cell* **20**, 21-32 (2005).

55. Wild, A.C., Yu, J.W., Lemmon, M.A. & Blumer, K.J. The p21-activated protein kinase-related kinase Cla4 is a coincidence detector of signaling by Cdc42 and phosphatidylinositol 4-phosphate. *J Biol Chem* **279**, 17101-10 (2004).

56. Stahelin, R.V., Karathanassis, D., Murray, D., Williams, R.L. & Cho, W. Structural and membrane binding analysis of the Phox homology domain of Bem1p: basis of phosphatidylinositol 4-phosphate specificity. *J Biol Chem* **282**, 25737-47 (2007).

57. Roy, A. & Levine, T.P. Multiple pools of phosphatidylinositol 4-phosphate detected using the pleckstrin homology domain of Osh2p. *J Biol Chem* **279**, 44683-9 (2004).

58. Yeung, T. et al. Receptor activation alters inner surface potential during phagocytosis. *Science* **313**, 347-51 (2006).

59. Schneiter, R. et al. Electrospray ionization tandem mass spectrometry (ESI-MS/MS) analysis of the lipid molecular species composition of yeast subcellular membranes reveals acyl chain-based sorting/remodeling of distinct molecular species en route to the plasma membrane. *J Cell Biol* **146**, 741-54 (1999).

60. Klemm, R.W. et al. Segregation of sphingolipids and sterols during formation of secretory vesicles at the trans-Golgi network. *J Cell Biol* **185**, 601-12 (2009).

61. Zhou, X. & Graham, T.R. Reconstitution of phospholipid translocase activity with purified Drs2p, a type-IV P-type ATPase from budding yeast. *Proc Natl Acad Sci U S A* **106**, 16586-91 (2009).

62. Devaux, P.F. Static and dynamic lipid asymmetry in cell membranes. *Biochemistry* **30**, 1163-73 (1991).

63. Wang, Y.J. et al. Phosphatidylinositol 4 phosphate regulates targeting of clathrin adaptor AP-1 complexes to the Golgi. *Cell* **114**, 299-310 (2003).

64. Costaguta, G., Duncan, M.C., Fernandez, G.E., Huang, G.H. & Payne, G.S. Distinct roles for TGN/endosome epsin-like adaptors Ent3p and Ent5p. *Mol Biol Cell* **17**, 3907-20 (2006).

65. Dobbelaere, J. & Barral, Y. Spatial coordination of cytokinetic events by compartmentalization of the cell cortex. *Science* **305**, 393-6 (2004).

66. Toenjes, K.A., Sawyer, M.M. & Johnson, D.I. The guanine-nucleotide-exchange factor Cdc24p is targeted to the nucleus and polarized growth sites. *Curr Biol* **9**, 1183-6 (1999).

FIGURE LEGENDS

Figure 1. PS distribution in budding yeast.

Distribution of (**a**) PS, monitored using the GFP-C2-Lact probe, (**b**) PI4,5P_2, monitored using the 2XPH-PLCδ-GFP probe and (**c**) the plasma membrane marker, Ras-GFP, during the cell cycle of BY4741 wild-type yeast cells grown to early log phase. In this and subsequent figures, images were acquired by spinning-disc microscopy. Images in **a-c** are representative of 3 experiments, with >50 cells analyzed per condition. (**d**) Quantification of the subcellular distribution of GFP-C2-Lact and 2XPH-PLCδ-GFP in cells with small buds (similar to cells in column iii), data are means ± S.E. ($n \geq 15$). Size bars = 4 μm.

Figure 2. Secretion is required for the polarized distribution of PS.

(**a**) Wild-type, *sec1^{ts}* and *sec6^{ts}* cells expressing GFP-Snc1 were grown to early log phase at 25°C, an aliquot shifted to 37°C for 30 min and images of live cells were acquired. (**b**) Wild-type, *sec1^{ts}* and *sec6^{ts}* expressing GFP-Lact-C2 were grown to early log phase at 25°C, an aliquot shifted to 37°C for 30 min and images of live cells acquired. (**c**) *Sec7^{ts}* cells co-expressing mRFP-Snc1 and GFP-C2-Lact were grown to early log phase at 25°C, an aliquot shifted to 37°C for 30 min and images of live cells acquired. Spinning disc confocal images are representative of 3 experiments, with >50 cells analyzed per condition. Dotted lines indicate juxtaposition of different fields from similar experiments. Size bars = 4 μm.

Figure 3. A recycling pathway supports the polarized distribution of PS.

(**a**) *Sec14^{ts}* cells co-expressing mRFP-Snc1 and GFP-Lact-C2 were grown to early log phase at 25°C, an aliquot shifted to 37°C for 60 min and images of live cells acquired sequentially. (**b**) *Sec14^{ts}* cells co-expressing Sec7-RFP and GFP-Lact-C2 were grown to early log phase at 25°C, an aliquot shifted to 37°C for 60 min and images of live cells acquired sequentially. (**c**) Parental and *rcy1Δ* cells co-expressing mRFP-Snc1 and GFP-Lact-C2 were grown to early log

phase at 25°C and live cell images acquired. Spinning disc confocal images are representative of 3 experiments, with >50 cells analyzed per condition. Dotted lines indicate juxtaposition of different fields from similar experiments. Size bars = 4 μm.

Figure 4. Photobleaching and fluorescence recovery of lipid-associated GFP.

Spinning-disc confocal images of wild-type cells expressing either (**a**) GFP-Lact-C2 or (**b**) GFP-RT just prior (left panels) and immediately after photobleaching (right panels). (**c**) Time course of recovery of GFP-C2-Lact (circles) and GFP-RT (squares) fluorescence after bleaching 2 μm spots, from experiments like those in **a-b**. Data are means ± S.E.M. of 6 individual FRAP determinations. Where absent, error bars are obscured by the symbol. (**d**) One-dimensional fluorescence intensity profiles along the plasma membrane were measured at the indicated times after photobleaching. The width of the initial area demarcated for bleaching is indicated by the dotted lines.

Figure 5. Phosphatidylserine is required for optimal Cdc42 location, activity and cell growth

(**a**) Wild-type and *cho1*Δ cells were grown to early log phase at 25°C. Equal numbers of cells were plated in 1:10 serial dilutions onto rich (YPD) agar and incubated at 25°C for 3 days**. (b)** Quantitation of bud emergence in wild-type (1607-5D) and the isogenic *cho1Δ* cells. Cells were grown to early log phase in rich medium containing galactose, harvested and arrested in G1 by incubating in rich medium containing glucose for 3 h. Next, cells were shifted back to galactose-containing medium. At the indicated times an aliquot of the culture was removed and fixed with 4% paraformaldehyde, cells were imaged using DIC microscopy and the percentage of budded cells counted. Graph displays percent of cells with new buds ± S.E.M. (n=3 with >100 cells counted per condition). * indicates $p < 0.025$ and ** indicates $p < 0.005$. (**c**) Wild-type and *cho1Δ* cells were transformed with p415MET-GFP-Cdc42 and grown in SC-leu medium

containing 400 μM methionine to allow for limited expression of the GFP-Cdc42 protein. Arrows indicate the buds in *cho1Δ* cells. (**d**) Wild-type and *cho1Δ* cells were transformed with a plasmid expressing Bem1-GFP. Arrows indicate the buds in the *cho1Δ* cells. Spinning disc confocal images in **c-d** are representative of 3 experiments, with >50 cells analyzed per condition. Due to the low signal of the Bem1-GFP 2x2 binning was used during image acquisition, accounting for the pixelated appearance of the images. Size bar = 4 μm.

Figure 6. Phosphatidylserine is required for the formation of mating projections.

(**a**) Wild-type and *cho1Δ* cells expressing GFP-Lact-C2 were grown to early log phase at 25°C and treated with mating factor α for 3 h before imaging. (**b**) Wild-type cells expressing GFP-PH-PLC (left) or the plasma membrane marker, Ras-GFP (right), were grown to early log phase at 25°C and treated with mating factor α for 3 h before imaging. (**c**) BY4741 or *cho1Δ* cells (10^6) were allowed to mate with SEY6210, Mat α cells (10^7). After 4 h the cells were resuspended in medium and serial dilutions were plated on medium selective for diploids. Mating efficiency was calculated as the percentage of input Mat **a** cells that formed diploids. Results are the average of 3 experiments with >1000 cells counted for each condition per experiment. (**d-g**) Confocal images of wild-type and *cho1Δ* cells expressing (**d**) GFP-Cdc42, (**e**) GFP-Cdc24, (**f**) Gic2-PBD-RFP and (**g**) Bem1-GFP following exposure to mating factor for 3 h. Spinning disc confocal images in **a,b,d-g** are representative of 3 experiments, with >50 cells analyzed per condition. Size bars = 4 μm.

Figure 7. Electrostatic interactions influence Cdc42 activity

(**a**) Phospholipid-recognition domains of Cdc42 and its effectors. This table, collating published data, shows the presence of established or potential anionic lipid-binding motifs or domains in Cdc42 and associated proteins. The relative affinity for PS and PI4P is shown, with ++

indicating strong binding, + indicating weaker, less-specific binding; ND = binding not determined. (**b**) Representative images of wild-type and *cho1Δ* cells expressing GFP-tagged tandem PH domains from OSH2, a probe for PI4P. (**c**) Wild-type and *cho1Δ* cells were transformed with pUG36-+8 expressing the surface charge probe GFP-+8. Spinning disc confocal images in **b,c** are representative of 2 experiments, with >50 cells analyzed per condition. Dotted lines indicate juxtaposition of different fields from similar experiments. Size bars = 4 μm.

SUPPLEMENTAL DATA

Strains, Plasmids, Growth Media and Genetic Methods

The rich medium used was yeast extract-peptone-dextrose (YPD; 10 g/liter yeast extract, 20 g/liter peptone, and 20 g/liter dextrose), and the minimal medium was synthetic dextrose (SD; 1.7 g/liter yeast nitrogen base without amino acids, 5 g/liter ammonium sulfate, 20 g/liter dextrose) containing the required nutritional supplements to complement strain auxotrophies and to ensure plasmid maintenance. For experiments involving the *cho1Δ* cells, minimal medium was supplemented with 1 μM choline. Bacto agar was added to the medium at 2% (wt/vol) prior to autoclaving to generate plates. Yeast strains were created using standard yeast and molecular biology procedures. Oligonucleotide synthesis and plasmid sequencing was performed by The Centre for Applied Genomics (Toronto, Ontario). A complete list of yeast strains used in this study is found in Supplementary Table 1 and a complete list of plasmids is found in Supplementary Table 2.

Plasmid construction

Plasmid pRS416-MET-GFP-Ras2 (CEN URA3) was constructed by PCR-amplifying the RAS2 gene using primers 5'-ClaI-Ras2 (5'- GCGATCGATATGCCTTTGAACAAGTCGAAC-3') and 3'-XhoI-Ras2 (5'- GCGCTCGAG TTAACTTATAATACAACAGCCACCC-3') and containing restriction enzyme sites for ClaI and XhoI to clone into pUG36 (a gift from J.H. Hegemann). Plasmid pRS416-MET-GFP-RT (CEN URA) was constructed by PCR-amplifying from base pair 861 to 969 of the RAS2 gene using primers 5'-ClaI-Ras2-(287) (5'-GCGATCGATGGTCAAGTTTCAAATGCTAAACAGGC-3') and 3'-XhoI-Ras2 (5'-GCGCTCGAGTTAACTTATAATACAACAGCCACCC-3') and containing restriction enzyme sites for ClaI and XhoI to clone into pUG36. Replacement of the *CHO1* gene with the KanMx cassette was performed by amplifying the deletion allele *cho1::kan*^{R} from the genome knockout

strain collection obtained from Open Biosystems by PCR using primers 5'-CHO1+450 5'-GCGATTTTTCCATTATAGCTC-3' and 3'CHO1+450 5'-TGCCTTTCTTTTTTTACACCC-3'. The linear product was transformed into yeast, and G418-resistant transformants were screened by PCR of genomic DNA for proper insert integration.

FRAP analysis

To determine the rate of recovery, the fluorescence intensity of the bleached area was compared to the intensity of an unbleached area of the plasma membrane. For each time point, the intensity of the bleached area was normalized to that of the corresponding unbleached area to correct for photobleaching incurred during the sampling. Data were fit to a simple diffusion, zero-flow model using the formula:

$$F_{(t)} = (F_{(t=0)} + F_{(t=\infty)} \text{ x } (t / t_{1/2})) / \ 1 + (t / t_{1/2})$$

where fluorescence intensity (F) at a given time (t) is related to the maximal fluorescence ($F_{(t=\infty)}$) and the half-time of maximal recovery ($t_{1/2}$). Using this equation, recovery curves were fit by least squares using Prism 4 (GraphPad Software, Inc.). Diffusion coefficients were calculated from the $t_{1/2}$ of the recovery curves as previously described using

$$D = (\omega^2/4\tau_{1/2})\ \gamma_D$$

where ω is the width of the bleach area, $\tau_{1/2}$ time of half-maximal recovery and γ_D a constant equal to 0.88.

Figure 1

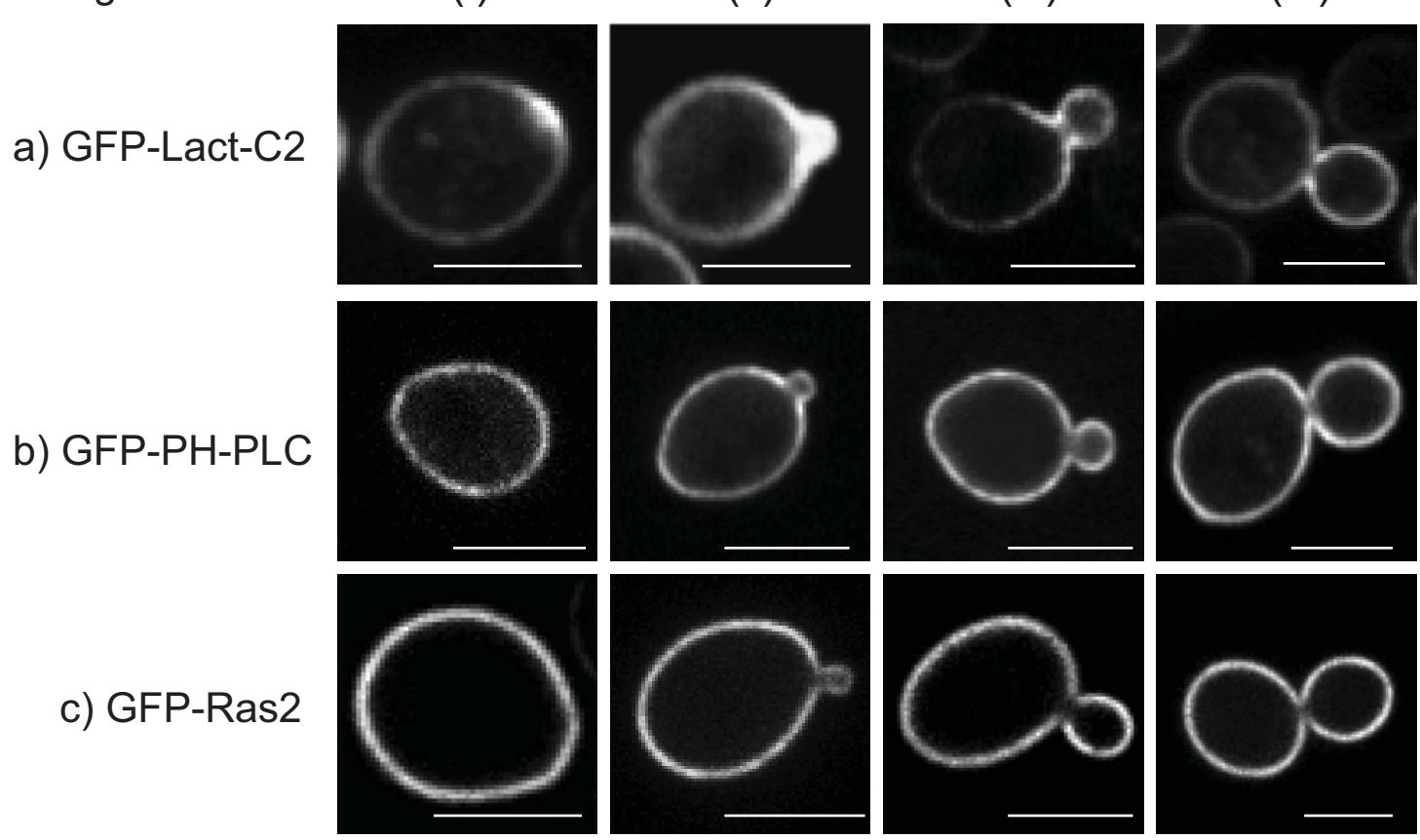
(i)
(ii)
(iii)
(iv)
a) GFP-Lact-C2
b) GFP-PH-PLC
c) GFP-Ras2

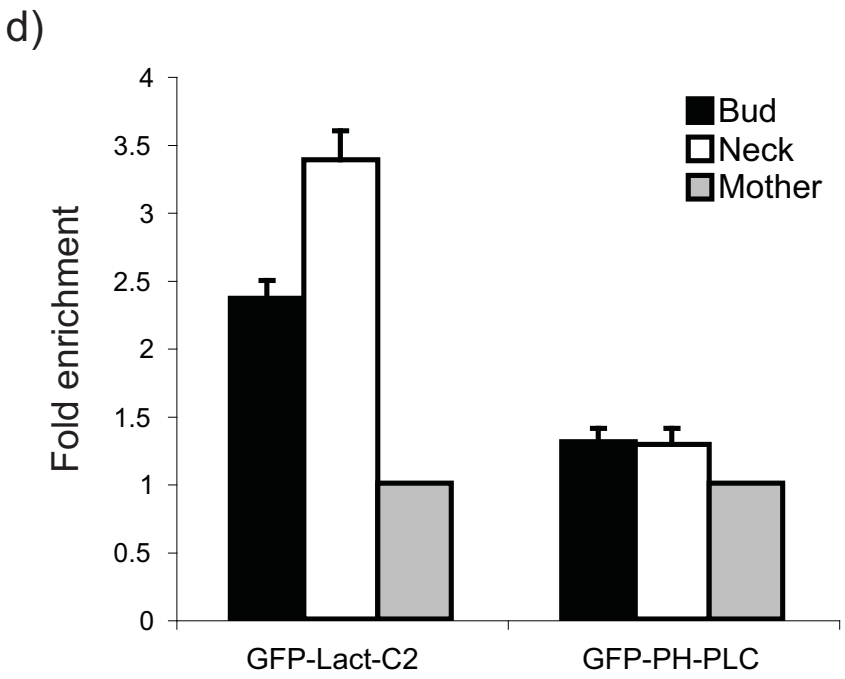
d)
Fold enrichment
4
3.5
3
2.5
2
1.5
1
0.5
0
Bud
Neck
Mother
GFP-Lact-C2
GFP-PH-PLC

Figure 2

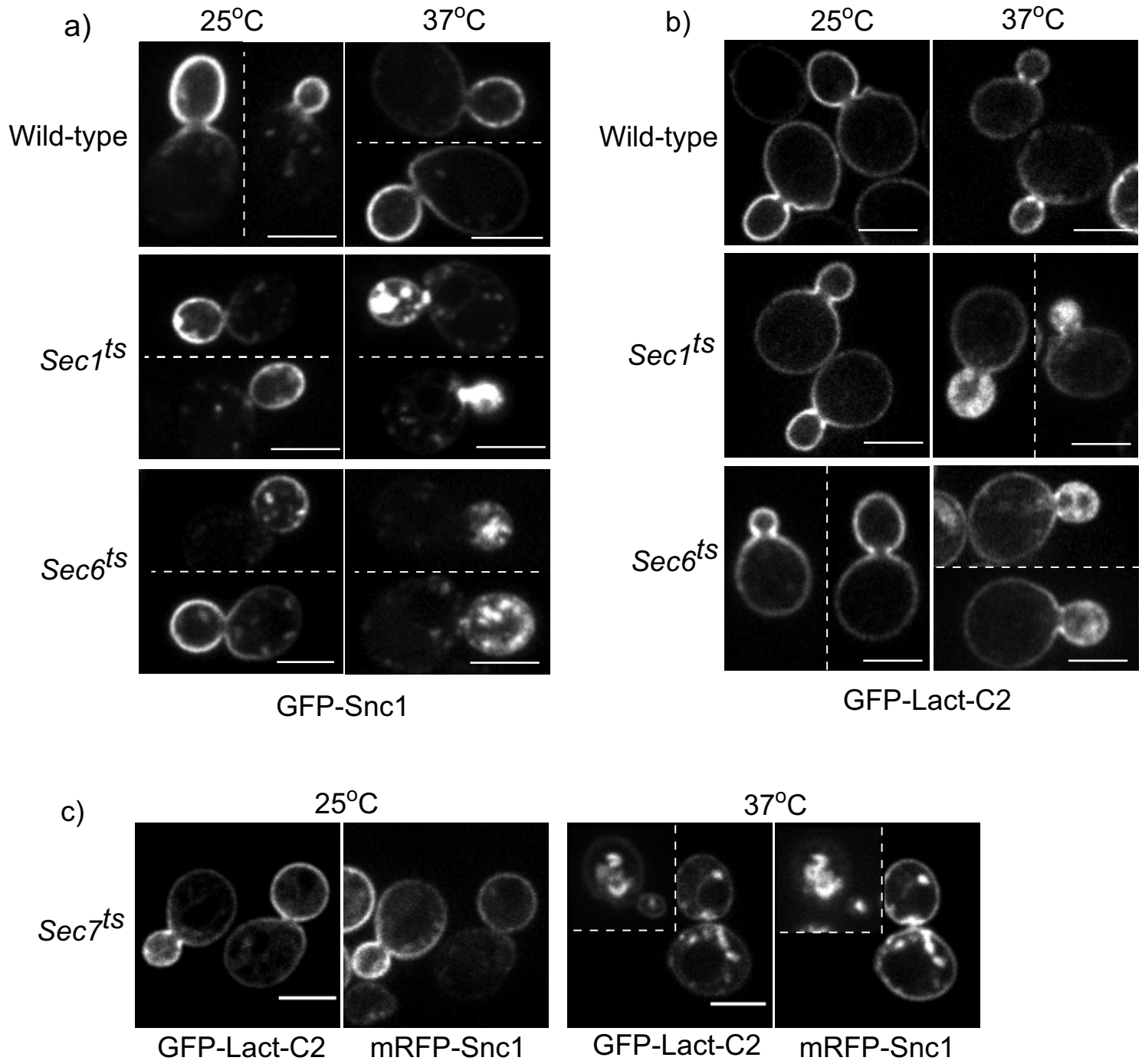
a)
25°C
37°C
Wild-type
Sec1ts
Sec6ts
GFP-Snc1
b)
25°C
37°C
Wild-type
Sec1ts
Sec6ts
GFP-Lact-C2

c)
25°C
37°C
Sec7ts
GFP-Lact-C2
mRFP-Snc1
GFP-Lact-C2
mRFP-Snc1

Figure 3

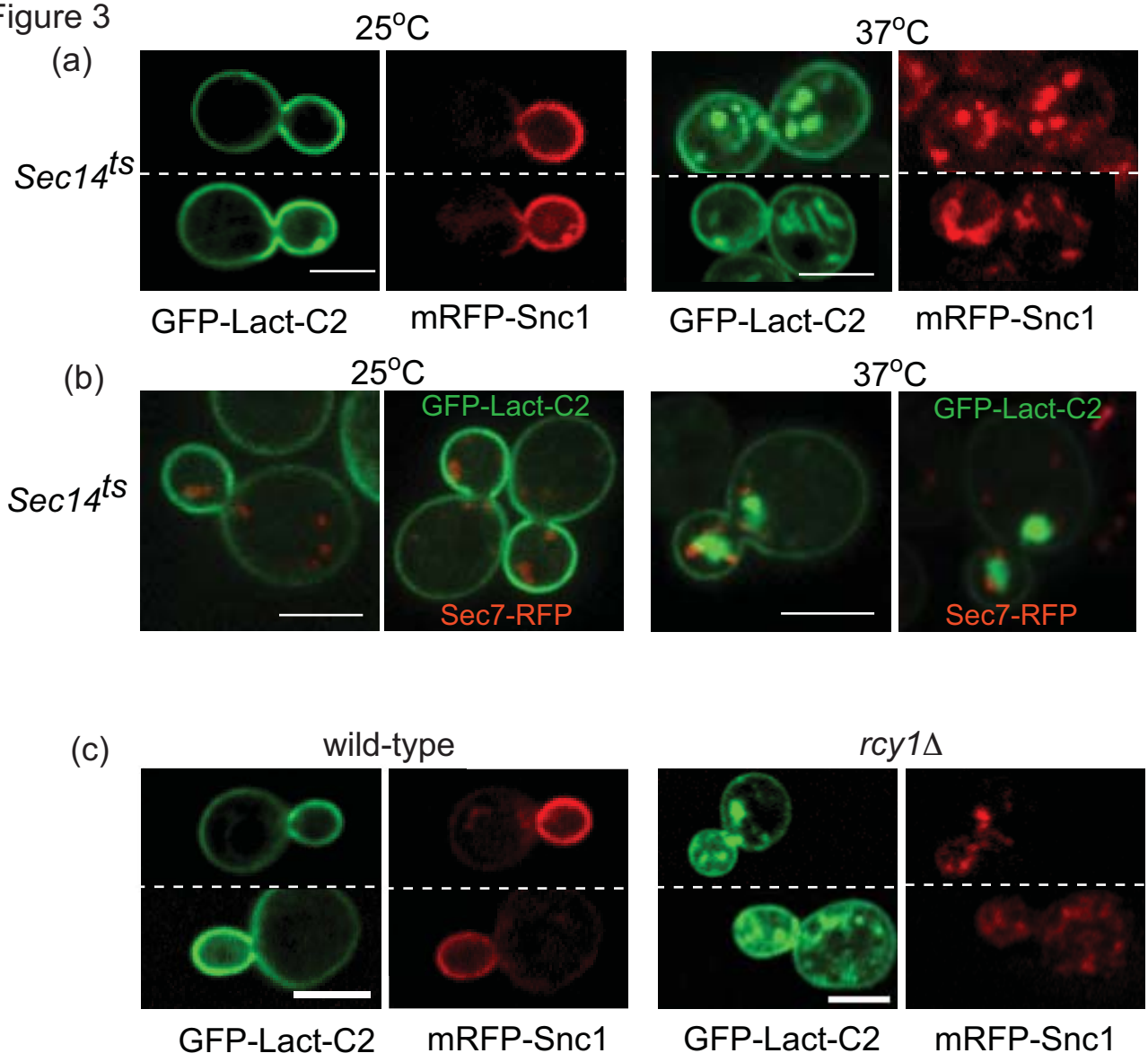
(a)
25°C
37°C
Sec14ts
GFP-Lact-C2
mRFP-Snc1
GFP-Lact-C2
mRFP-Snc1
(b)
25°C
37°C
Sec14ts
GFP-Lact-C2
Sec7-RFP
GFP-Lact-C2
Sec7-RFP
(c)
wild-type
rcy1Δ
GFP-Lact-C2
mRFP-Snc1
GFP-Lact-C2
mRFP-Snc1

Figure 4

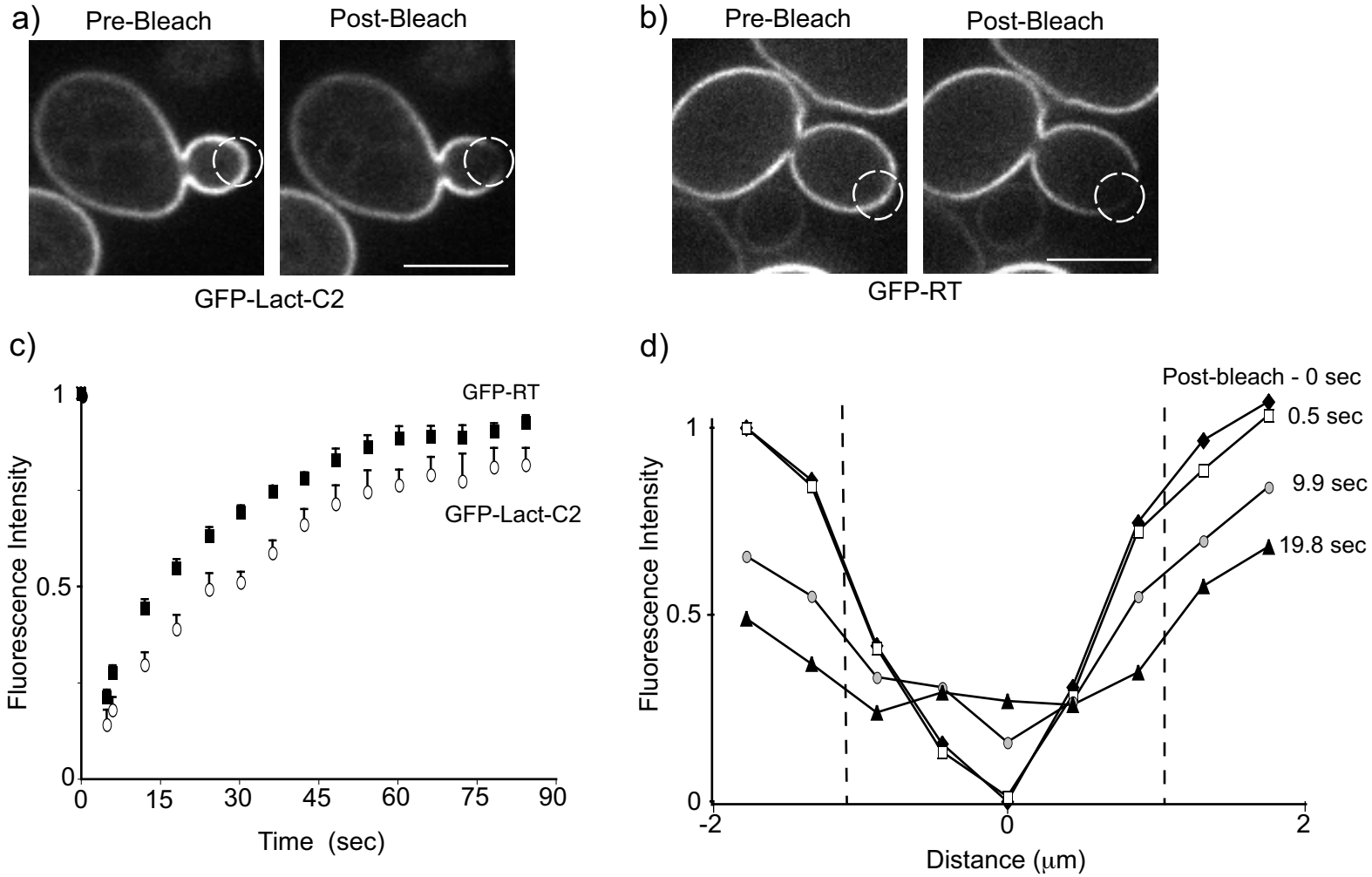
a)
Pre-Bleach
Post-Bleach
GFP-Lact-C2
b)
Pre-Bleach
Post-Bleach
GFP-RT
c)
GFP-RT
GFP-Lact-C2
Fluorescence Intensity
Time (sec)
d)
Post-bleach - 0 sec
0.5 sec
9.9 sec
19.8 sec
Fluorescence Intensity
Distance (μm)

Figure 5

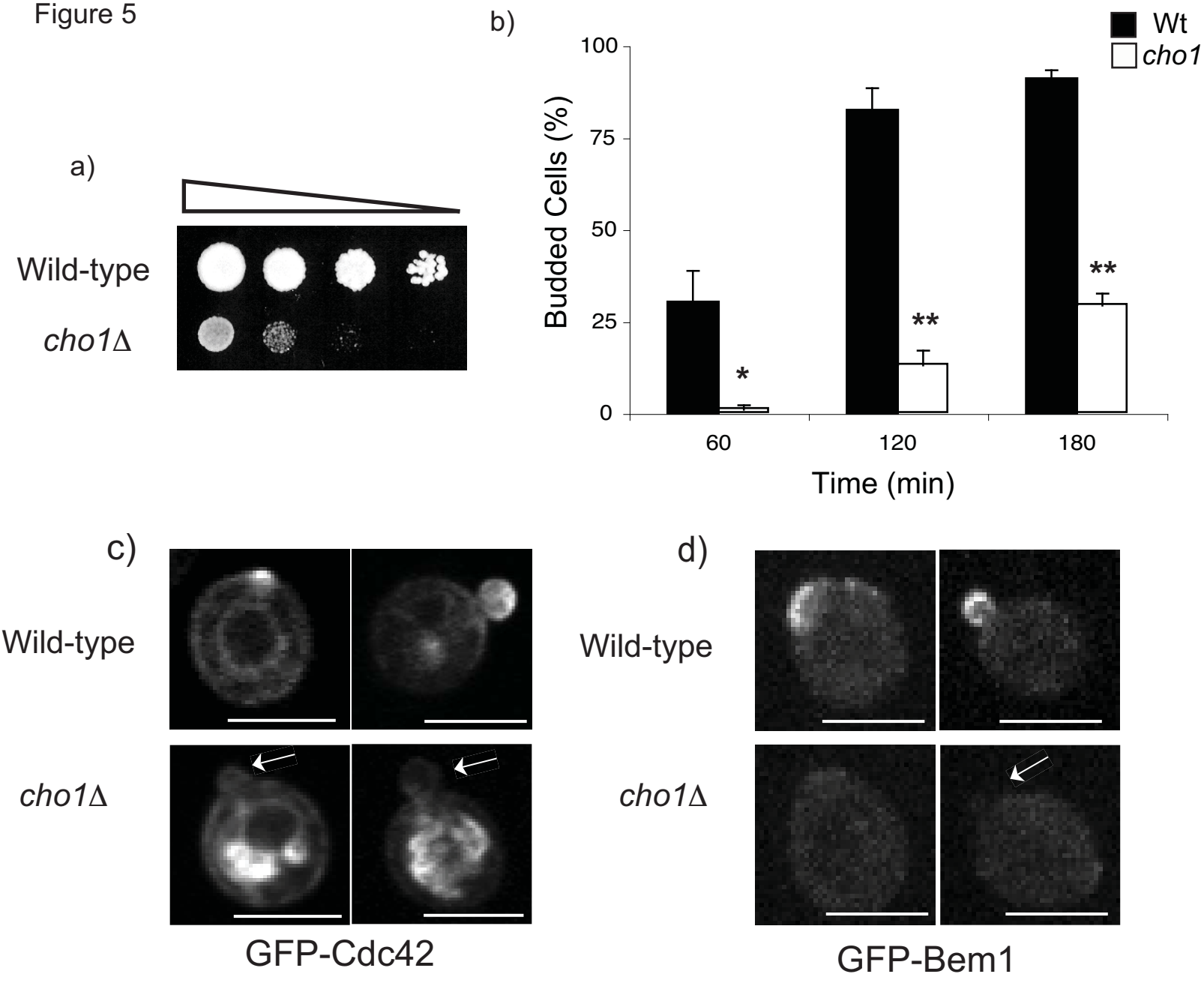
a)
Wild-type
cho1Δ
b)
Wt
cho1
Budded Cells (%)
100
75
50
25
0
*
**
**
60
120
180
Time (min)
c)
Wild-type
cho1Δ
GFP-Cdc42
d)
Wild-type
cho1Δ
GFP-Bem1

Figure 6

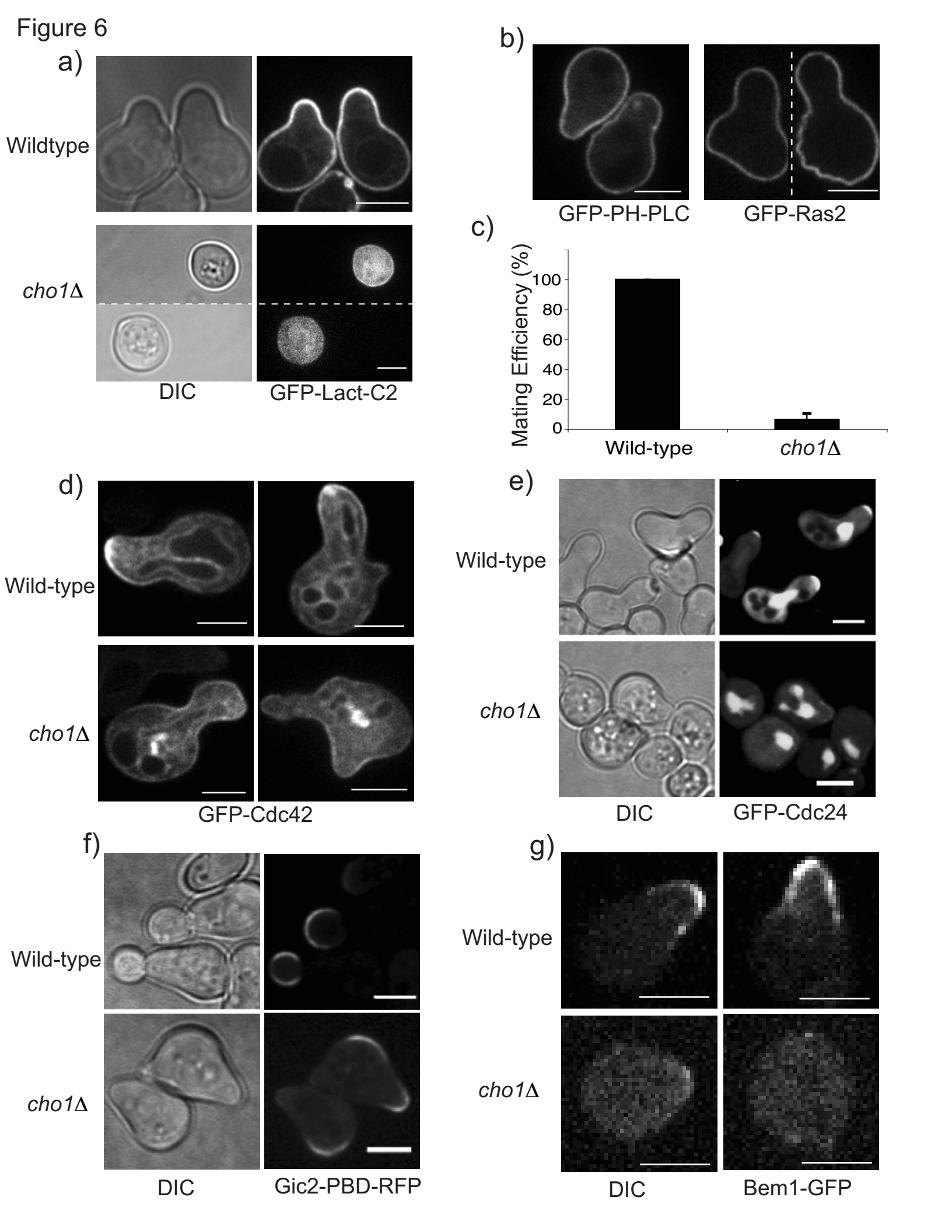
a)
Wildtype
cho1Δ
DIC
GFP-Lact-C2
b)
GFP-PH-PLC
GFP-Ras2
c)
Mating Efficiency (%)
100
80
60
40
20
0
Wild-type
cho1Δ
d)
Wild-type
cho1Δ
GFP-Cdc42
e)
Wild-type
cho1Δ
DIC
GFP-Cdc24
f)
Wild-type
cho1Δ
DIC
Gic2-PBD-RFP
g)
Wild-type
cho1Δ
DIC
Bem1-GFP

Figure 7

a)

	Motif	PS	PI4P	
Cdc42	polybasic	ND	ND	
Cdc24	PH	ND	ND	
Bem1	PX	+	++	Stahelin et al.,
Cla4	PH	+	-	Wild et al.,
Ste20	polybasic	+	+	Takahashi et al.,
Gic1	polybasic	+	+	Takahashi et al.,
Gic2	polybasic	+	+	Takahashi et al.,
Rsr1	polybasic	ND	ND	
Ste5	polybasic	ND	+	Winters et al.,

b)

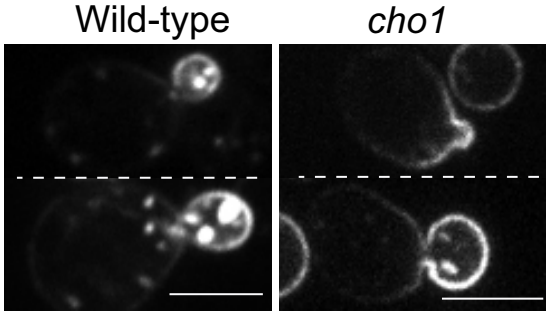

c)